Including Convective Flows in a Self-Consistent Hydrogen-Based

Founded 1855 VERS

Microwave PACVD Reactor Model

C. S. Meierbachtol¹, T. A. Grotjohn¹, B. Shanker^{1,2}





Motivation

- Higher pressures for Microwave PACVD reactors result in:[1]
- 1. Faster growth rates
- 2. Better quality diamond
- Development of multi-physics simulations at higher pressures will:
- Help understand underlying mechanisms
- Aid in development of new reactors

Governing Equations

Electromagnetics (FDFD)

$$\left[\nabla \times \frac{1}{\hat{\epsilon}_{\mathbf{r}}} \nabla \times - \left(\frac{\omega}{c}\right)^2\right] \vec{H} = 0 \tag{1}$$

Absorbed Power

$$\mathcal{P} = \frac{1}{2} \Re\{\sigma_e\} \left(\vec{E} \cdot \vec{E}^* \right) \tag{2}$$

Plasma

$$\nabla \left(\rho \frac{M_s}{M} D_s \nabla x_s \right) = W_s - \nabla \cdot (\rho_s \vec{v}) \tag{3}$$

$$-\frac{\partial v_r}{\partial t} = v_r \frac{\partial v_r}{\partial r} + v_z \frac{\partial v_r}{\partial z} + \frac{1}{r\rho} \frac{\partial p}{\partial r} + \frac{1}{r\rho} \frac{\partial (r\tau_{rr})}{\partial r} + \frac{1}{\rho} \frac{\partial \tau_{rz}}{\partial z}$$
 (4a)

$$-\frac{\partial v_z}{\partial t} = v_r \frac{\partial v_z}{\partial r} + v_z \frac{\partial v_z}{\partial z} + \frac{1}{r\rho} \frac{\partial p}{\partial z} + \frac{1}{r\rho} \frac{\partial (r\tau_{rz})}{\partial r} + \frac{1}{\rho} \frac{\partial \tau_{zz}}{\partial z} - g$$
(4b)

$$\nabla \cdot \lambda_{g} \nabla T_{g} = \nabla \cdot \left[\rho \vec{v} \left(\frac{1}{2} v^{2} + \frac{3k_{B} T_{g}}{2m_{0}} \right) \right] =$$

$$\nabla \cdot \left(\lambda_{e} \nabla T_{e} + \lambda_{v} \nabla T_{v} + \sum_{s=1}^{N_{s}} \rho h_{s} D_{s} \nabla x_{s} \right)$$

$$- \nabla \cdot (p \vec{v}) + \nabla \cdot \hat{\tau} + \mathcal{P}_{abs} - Q_{rad} + n \vec{g}$$
(5)

Conductivity

$$\sigma = \frac{q_e^2 n_e}{m_e} \left(\frac{\nu_{eff} - j\omega}{\nu_{eff}^2 + \omega^2} \right) \tag{6}$$

Geometry

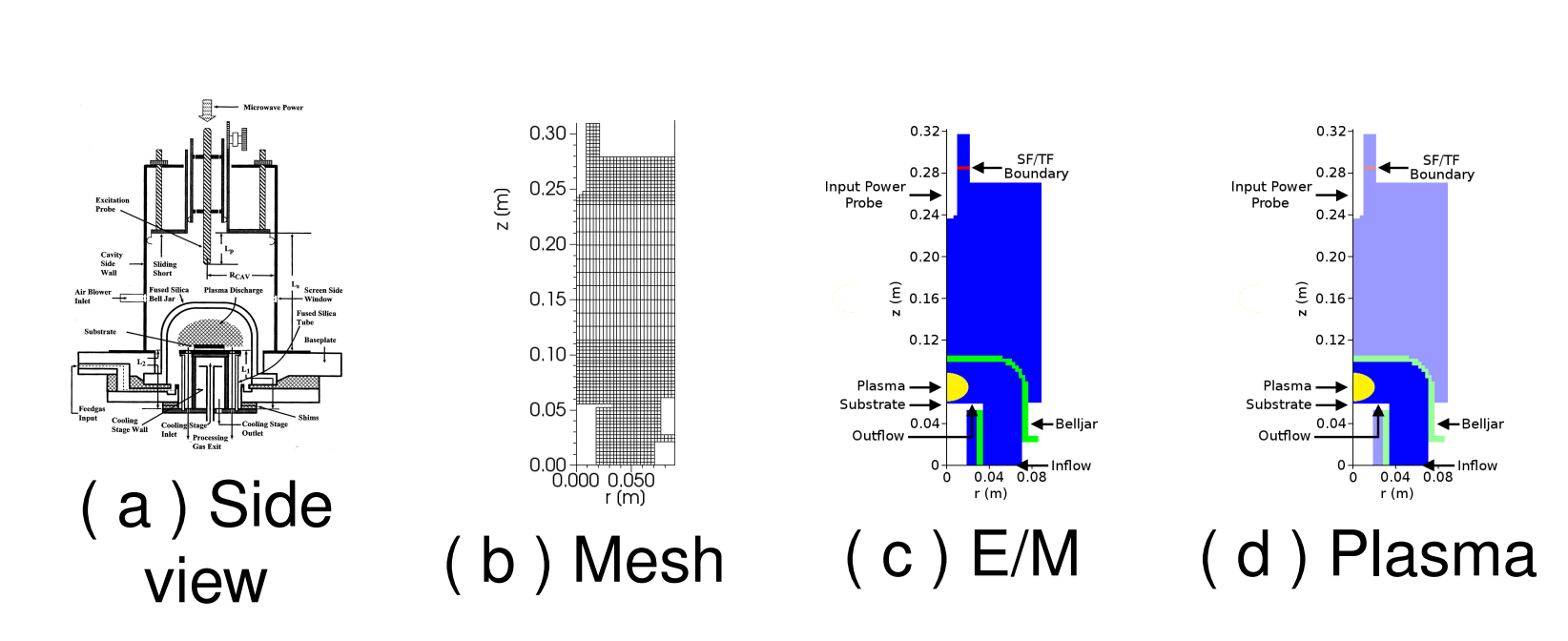


Figure 1: (a) Schematic of MSU Microwave PACVD reactor, (b) discretized mesh, (c) electromagnetics and (d) plasma simulation domains.

Solution Process

- Electromagnetics: Direct (sparse)
- Plasma (Scalar): Gauss-Seidel Line Relaxation
- Plasma (Flows): Implicit direct solver [2]

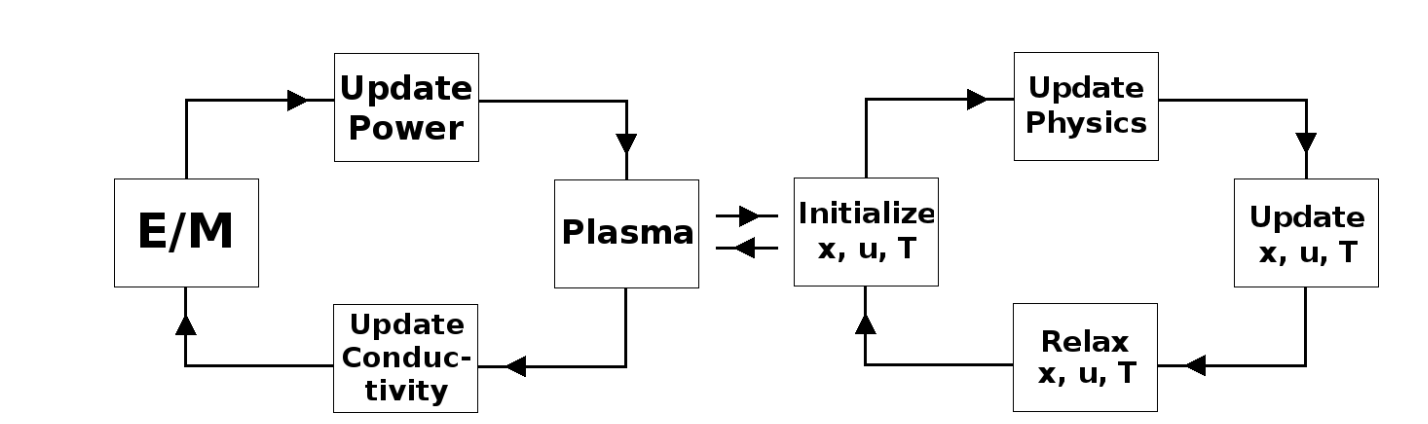


Figure 2: Solution process for (left) complete system and (right) plasma convergence.

Validation

Electron Density

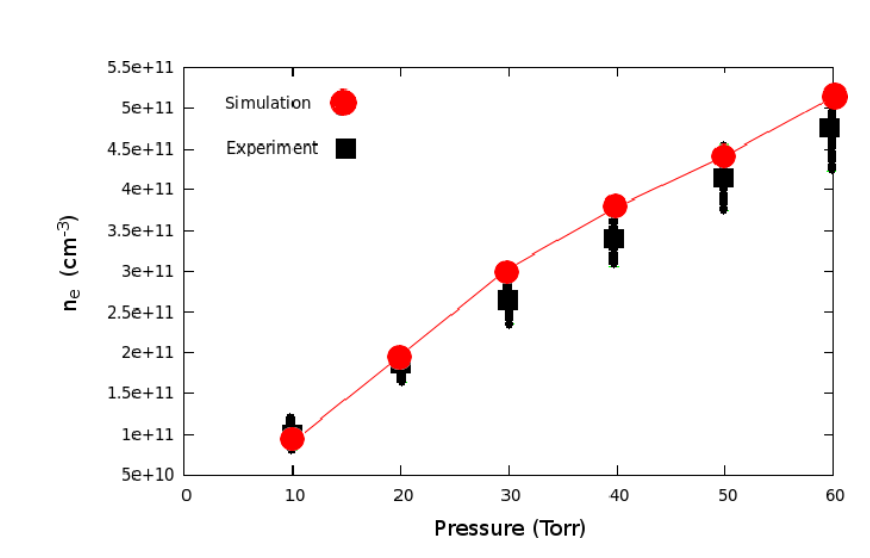


Figure 3: Simulated (red) and experimentally measured (black) electron density versus pressure at constant power of 600 Watts. Experimental data from Grotjohn et. al., 2000.

High Pressure Results

Electromagnetic Module

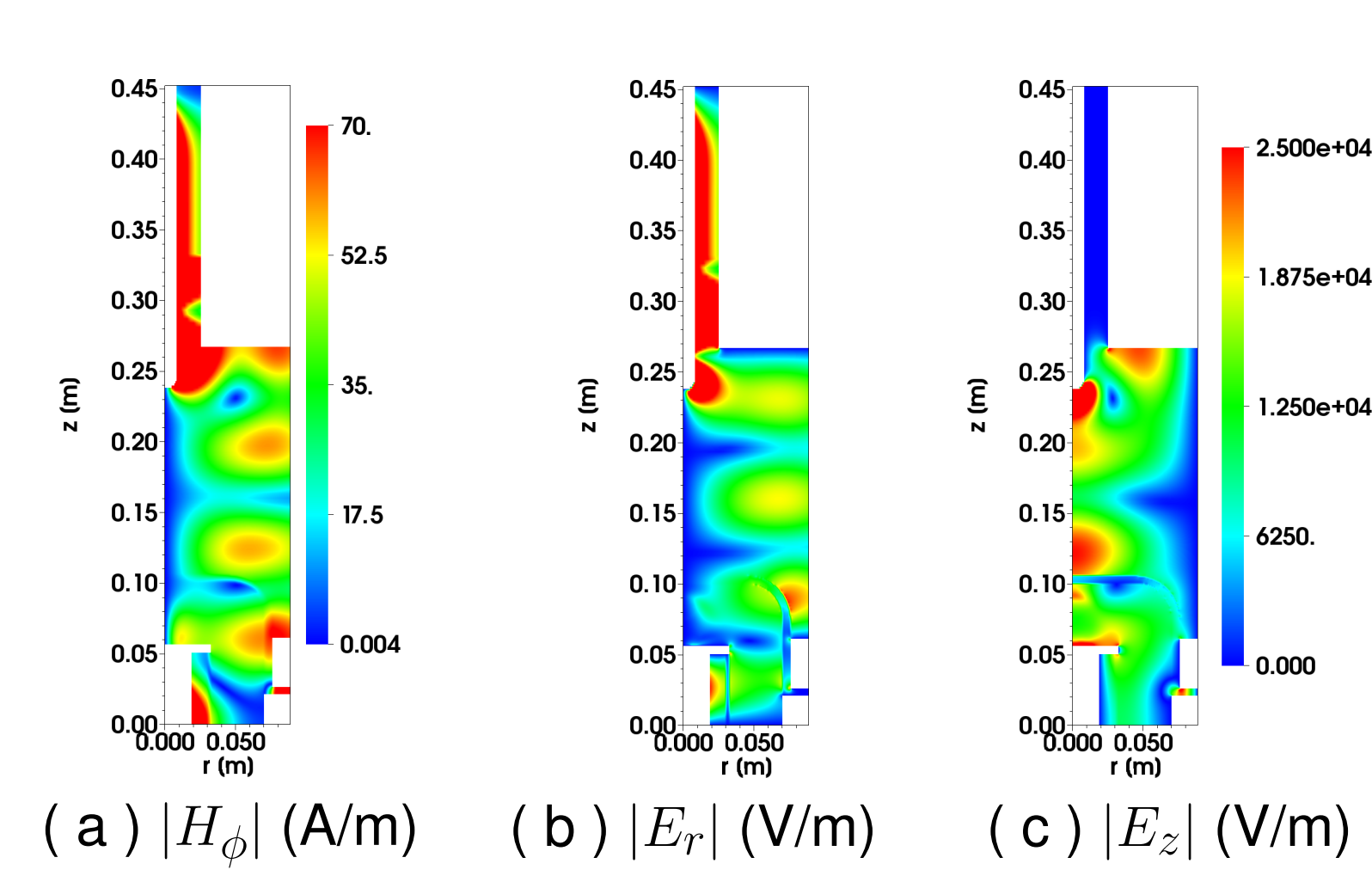


Figure 4: (a) $|H_{\phi}|$, (b) $|E_r|$, and (c) $|E_z|$ solutions when operating at 250 Torr and 3 kW. The same scale is used in both electric field plots.

Plasma Flow Module

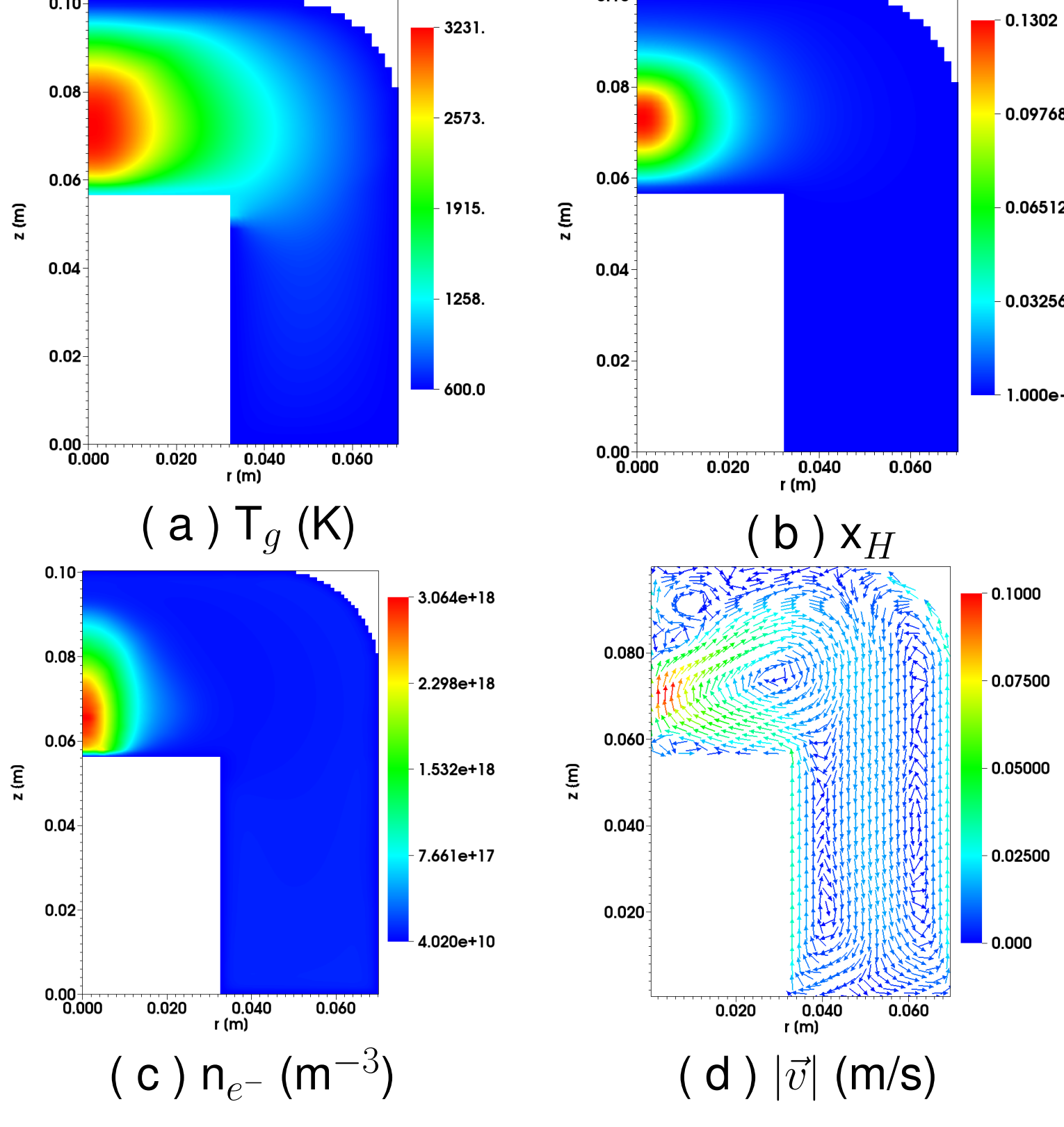


Figure 5: MSU reactor (a) gas temperature, (b) H molar fraction, (c) electron denisty, and (d) vector gas flow for \mathcal{P}_{abs} of 3 kW and pressure of 250 Torr.

Convective Flow

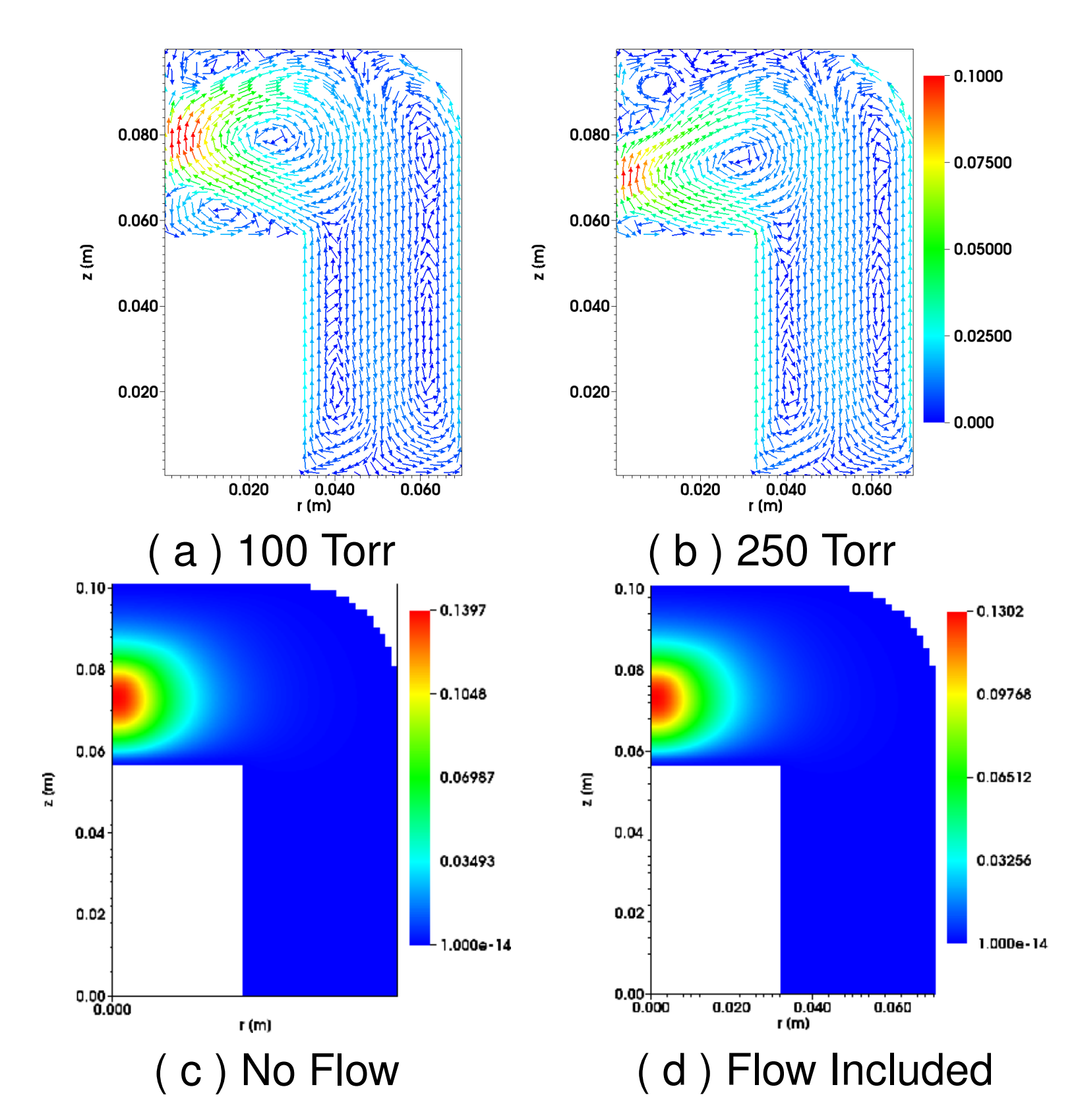


Figure 6: Average gas flow vector at (a) 100 Torr, 1.5 kW and (b) 250 Torr, 3 kW, and atomic hydrogen mole fraction for (c) no flow and (d) flow included at 250 Torr, 3 kW.

Conclusions

- Self-consistent multi-physics Microwave PACVD diamond reactor simulation accurate at higher pressures
- Convective forces significant above 150 Torr
- Influence primarily in mole fractions
- Future work:
- Substrate temperature
- Hydrocarbons

References

- [1] K.W. Hemawan, T.A. Grotjohn, D.K. Reinhard, and J.Asmussen, Diam. Rel. Mater. **19**, 1446-1452 (2010).
- [2] Gilbert Strang, Computational Science and Engineering (2007).